AD-A193 538 HIERARCHICAL STRUCTURE IN POLYMERIC SOLIDS AND ITS INFLUENCE ON PROPERTIES(U) BRISTOL UNIV (ENGLAND) A KELLER MAR 88 DAJA45-85-C-0004 1/1

UNCLASSIFIED F/G 7/3 NL

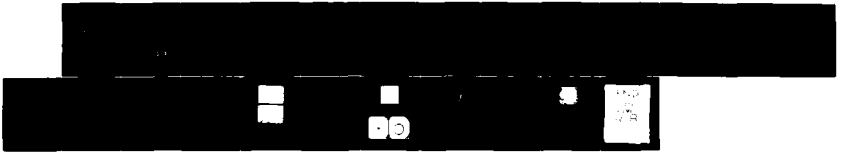

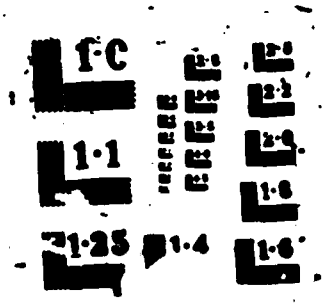
1.C
1.1
1.25
1.4
1.6

barkel (1.25)

AD-A193 538

HIERARCHICAL STRUCTURE IN POLYMERIC SOLIDS AND ITS INFLUENCE ON PROPERTIES

Investigator: A. Keller

Contractor: Department of the U.S. Army, ERO

Contract Number: DAJA45-85-C-0004

6th Periodic Report*

September 1987 - March 1988

The Research reported in this document has been made possible through the support and sponsorship of the U.S. Government through its European Research Office of the U.S. Army. This report is intended only for the internal management use of the Contractor and the U.S. Government.

*5th on work performed

Summary

Of the variety of avenues arising from our preceding investigations of Professor Percec's (Cleveland) specially synthetized mesogenic polyethenes, currently we pursued the aspect of non-equilibrium liquid crystal deficiency ("degree of (non-equilibrium) liquid crystallinity"); and its perfectioning on heat treatments. We established and compared the effect of heat treatments both when annealed while in the liquid crystalline and in the crystalline solid state with numerous implications arising. We investigated effects related to non-equilibrium liquid crystal deficiency as a function of chain flexibility and molecular weight (M). We observed, amongst others, that increased flexibility reduces this deficiency and promotes perfectioning when such deficiency is present, while decreasing flexibility and increasing M has the opposite effect with the outcome that variability of "degree of liquid crystallinity", as normally observed, is most pronounced at intermediate flexibilities and molecular weights. These and similar other features should be important for designing new liquid crystal polymers, and once obtained, for their characterisation.

The second part of the programme was aimed at registering orientation in lyotropic PBT in situ. In the particular instance the study was focussed on the relaxation from the highly oriented state, a crucial stage in the processing of liquid crystal materials as regards ultimate properties of the final product. Presently, an X-ray method was developed to supplement and eventually supersede previous birefringence work. Thanks to access to high intensity synchrotron X-source and to newly developed programmes of computational data handling we could now follow the actual reorientation process through diffraction effects arising from the inherent periodicity of the rigid rod molecule. These developments create unique new possibilities to be exploited. Further, unexpectedly, also solvent orientation effects became apparent offering new handles towards solvation and polymer-solvent interaction, important issues for such stiff, poorly soluble polymers.

Finally, we recognized that we possess the potential to register stress within the molecules by Raman spectroscopy in externally loaded samples. Thus we should be able to map local stress distributions using molecules as strain gauges in heterogeneous samples down to optical resolution limit of the structure hierarchy. The technique is now being applied to a variety of polymers of which PBT falls within the present programme. New potentials arising also feature in proposal for future work submitted during the current period [1].

INTRODUCTION

Work during the present period was centred on two different subject areas each involving different types of materials.

I) The first involved the family of polyethers synthetized by Professor Percec and focussed on the issue of non-equilibrium liquid crystal deficiency discovered during the last period using these compounds [2,3].

II) The second line was on the fully rigid-rod lyotropic polymer PBT and centred on its orientability.

III) The third line is the spectroscopic registration of localized molecular stresses.

I) For this part of the programme as before, the materials consist of rigid mesogen and flexible spacer sequences (with variable spacer lengths) combined through ether linkages. To recapitulate, the compounds are

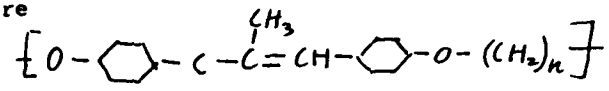

where n is a variable (5,7,9, or 11, homopolymers, or alternately 5 and 7 or 9 and 11 copolymers). The unique advantages of these materials for our purposes have been laid our previously.

Work during the present period continued to take advantage of the opportunities offered by these Cleveland materials. However, the subject matter addressed was somewhat more restricted than previously as it was circumscribed by amounts and type available while awaiting new consignments currently being dispatched. The subject intensively embraced, relying on this class of material, was based on our previous recognition that the temperature and heat of isotropization was affected by the preceding thermal treatment of the system, leading to the recognition of non-equilibrium liquid crystal deficiency, manifest also in terms of optically visible microstructure. Present investigations were aimed to consolidate these first recognitions and explore the dependence of the effects on the conditions of heat treatments (temperature, time) and on the nature of the compounds, namely degree of chain flexibility (flexible spacer type and composition ratios) and on molecular weight.

II) PBT (poly-p-phenylbenzthiazole) is a lyotropic fully rigid chain with formula

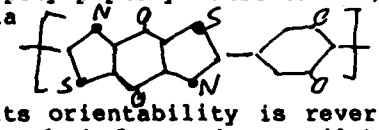

Examination of its orientability is reverting to our initial main line programme (proposed before the availability of Professor Percec's compounds arose). To extend the previously initiated work relying on orientation mapping by birefringence, we have now explored the possibility of invoking also the potentially much more informative X-ray method. Applicability of this method in the dilute lyotropic state, and this for following transient effects in real time, was by no means self evident. However, thanks to access to a synchrotron X-ray source and use of sophisticated computerized data-processing programmes the method is now established awaiting exploitation.

III) The possibility to register localised molecular stresses by Raman spectroscopy down to the level of the limit of resolution of optical microscopy, thus opening the way for mapping stress distributions using molecules as strain gauges in terms of the microscopic structure hierarchy, arose unexpectedly. It arose through the confluence of developments elsewhere [4], and our acquisition of appropriate equipment. We set out to exploit this unique opportunity in aid of correlating studies on structure with those on properties with particular reference to hierarchical nature of polymeric matter. Amongst the first, were tests carried out on PBT thus dovetailing with the rest of our work on PBT, but with much further potential beyond this particular material.

I. NON EQUILIBRIUM LIQUID CRYSTAL DEFICIENCY

Background and Objectives

To quote from the preceeding report: "It was found, while mapping the isotropic→liquid crystal phase transitions in Professor Percec's polyethers that, even when confined to the thermotropic state, the isotropization temperature (T_i) could not be uniquely identified just by a simple heating or cooling run in the DSC or under the optical microscope, because there were variations from run to run and/or sample

to sample. It was observed that, just as in the case of crystalline polymers, the value of T_i is affected by the thermal history of the sample accompanied by optically visible texture changes in the microstructure characterizing the liquid crystalline state. This recognition, which to our knowledge has no precedent, should have wider ranging consequences. Consequently, somewhat departing from our initial objective we set out to examine this effect more specifically. As a result it became possible to identify and characterize quantitatively non-equilibrium liquid crystal deficiency, analogously to the familiar degree of crystallinity determinations in the crystalline state of semi crystalline polymers in the expectation of correlating this ..... with features of the microstructure on the optical level of the structure hierarchy".

The work during the present period emanates from the stage reached previously and expressed by the above quoted statement. At this point two diagrams are required to convey the factual and conceptual background.

Fig. 1, shown previously and recapitulated here for clarity, displays three transition temperatures: glass transition (T_g) crystal melting (T_m^{max}) and isotropization (T_i) as a function of molecular weight ($\bar{M}_n$). (T_m^{max} is the maximum obtainable by annealing each preparation so as to give stablest crystal). As anticipated, all three transitions first increase then level off with $\bar{M}_n$. However, the T_i-s above $\bar{M}_n$ = 12000 become multivalued. It did turn out that this variability is affected by preceding thermal history of the samples. Basically this means that the as measured T_i is not, as is generally believed, an equilibrium quantity.

As a result of considerations during the present period we are expressing conditions through the free energy-temperature diagram in Fig. 2. Here, at any given T, the state of lowest free energy is that of lowest G, i.e. below T_i^{∞} (the equilibrium isotropization temperature after infinite time of heat treatment - see below)it is the nematic liquid crystalline state, and above T_i^{∞} it is the true isotropic liquid. Analogously, T_m^{max} defines the temperature at which the true crystal transforms into liquid crystal. The dashed line in Fig. 2 represents the free energy of one non-equilibrium liquid crystal state, the possible existence of which is our new recognition. This gives a temperature of isotropization, $T_i < T_i^{\infty}$, the result of direct measurement which, short of our recent recognition would have been taken as the true thermodynamically defined liquid-crystal→liquid transition temperature. The immediate issues arising therefore are: the identification of the true T_i^{∞} for a given material and ΔG, the departure from equilibrium for a particular material under specific treatment conditions. At this stage the former we do numerically, while the latter by registering trends. It is most important to point out (as otherwise it is likely to give rise to misunderstandings) that here we are referring to non-equilibrium disordered liquid crystal states which is distinct from equilibrium disorder always present and usually characterized by an order parameter, a quantity which changes reversibly with T in the temperature range $T_m^{max} < T < T_i$. It is to be noted that this is a decreasing function of T in contrast to the non-equilibrium disorder which has the opposite temperature dependence.

Effect of Molecular Weight

Regarding trends, that of dependence on molecular weight is already apparent from Fig. 1 supported by new data on copolymer 5,7 recently acquired. For low molecular weights ($\bar{M}_n$ <12000) non-equilibrium liquid crystal states are not noticeable; clearly here the material is sufficiently mobile to equilibrate (at least on the time scale of usual

heating and cooling rates) just as in low M liquid crystals. $T_i^{\infty} - T_i$ becomes sizeable for $\bar{M}_n = 17000$. Fig. 3 shows how T_i increases towards T_i^{∞} with the time of the annealing treatment (see below). For the highest M-s available ($M_n = 33000$) however the departure from the apparently final T_i value is smaller again. We now have reason to think that the point for $\bar{M}_n = 33000$ in Fig. 1 is still below T_i^{∞} which thus is not yet reached; accordingly the true T_i^{∞} should be still higher, a point currently being pursued. The trend which emerges therefore is that departures from equilibrium liquid crystal perfection are increasing with M, but nevertheless will become most noticeable at intermediate M-s where the mobility of the chains is sufficiently slow to yield non-equilibrium states, but still high enough to respond to commonly occurring variations in sample treatments.

It is important to state here that all heat annealing treatments with copolymer 5,7 (featuring in Figs 1 and 3) were carried out in the crystalline state, i.e. below T_m^{max} (to avoid degradation which was experienced at the high temperature above T_m^{max} for the long holding times needed). While remarkable that this had an effect on T_i at all (see below) it was insufficient for asserting that the liquid crystalline state can be perfected in itself directly through heat treatment. To eliminate this uncertainty in works to follow heat treatments were performed in the liquid crystal range (i.e. between T_i and T_m^{max}) itself. To reduce the risk of degradation we turned to another copolymer pair (9,11) for making the principal point that the liquid crystal state can be perfected by heat treatment in situ. This polymer had lower transition temperatures, and as we found (see later) showed higher rates of reorganization, hence required shorter holding times. The material available for this work had $\bar{M}_n = 30800$.

Annealing above T_m^{max}; effects of chain flexibility

Fig. 4a shows DSC thermograms corresponding to the isotropization transition as a function of heat treatment time above T_m^{max}. As seen, both the temperature (T_i) and the heat (ΔH_i) of isotropization, the former as assessed from the position and the latter from the area of the endothermic peak, are increasing with annealing time. The variation of T_i and ΔH_i with annealing time (t) are displayed in Figs. 5 and 6.

By assuming an exponential approach of T_i to T_i^{∞} and of ΔH_i to ΔH_i^{∞}, and by linearizing $\ln(T_i^{\infty} - \Delta H_i(t))$ and $\ln(\Delta H_i^{\infty} - \Delta H_i(t))$ respectively this extrapolates to 171.6°C for T_i^{∞} and to 11.2J/g for ΔH_i^{∞}. With the latter we can then define $\Delta H_i(t)/\Delta H_i^{\infty}$ which we term the "non-equilibrium degree of liquid crystallinity", also plotted in Fig. 6 (see below). It needs noting, however, that the linearisation is not satisfactory all along the curves: in particular, the procedure makes the curve lie too low in fig. 5 and explicitly "rejects" the first (unannealed) point in Fig. 6 (not shown). These 'misfits' demonstrate that the full process of perfectioning cannot be represented by a single exponential, and more explicitly, that initially it follows a much faster exponential than later on, a deduction of interest for the mechanism of perfectioning (see below). However, as the second slower exponential dominates most of the later points, the reliability of the extrapolation, hence the values of T_i^{∞} and ΔH_i^{∞} arrived at above, remains unimpaired.

Fig. 7 displays the polarising optical images in 2 stages of sample annealing. The coarsening of the grainy texture with increasing annealing time is apparent, even if not as strikingly as it has been for copolymer 5,7 (previous report).

Finally, under the present heading, it will only be stated that a side chain polyether from Prof. Percec was also investigated regarding non-equilibrium defects in liquid crystallinity. The compound was a polypropylene backbone with an ether side group of

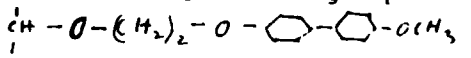

No evidence for any deficiency in "degree of liquid crystallinity" was found by our present DSC evidence: namely the isotropization endotherm was unaltered by heat treatments both as regards position and peak area.

Some Interim conclusion

At this stage we may draw the following interim conclusions about factors influencing "non-equilibrium liquid crystallinity".

i) We can assert the existence of non-equilibrium liquid crystal deficiencies, their reduction and eventual removal by heat annealing in the liquid crystalline state itself. This is in addition to the previously established influence of the crystalline state on the subsequently formed liquid crystal state arising therefrom (the end-state of the latter is represented by the dashed line endotherm in Fig. 4a: we see that the two end states, the ones resulting from liquid crystal and solid state annealing, are closely similar). Conversely, the previous observation that heat treatment of the true crystal affects the degree of liquid crystallinity on subsequent heating above T_m is notable in itself: namely, it requires large scale rearrangement in the crystal texture on heat treatment, in the range of microns, i.e. perfectioning of the mutual arrangement of texture elements in the optical microscope range of the structure hierarchy. We know that this must be so, because by prevous DSC evidence the thermal stability of the crystals themselves (on the lattice level) is not affected by heat treatments such as do influence the state of subsequent liquid crystallinity. The suggestion of crystal perfectioning on such a large scale is new, with many further potential consequences.

ii) Perfectioning is more pronounced and faster for 9, 11 than for 5,7; and is faster and more significant for copolymers than for homopolymers (Fig. 4b) to be commented on more specifically below; it is altogether absent for side chain polymers. This is consistent with the perfectioning being promoted by higher overall mobility (the longer flexible spacers in the 9,11 copolymers are more mobile). Also the side group in the side chain LC polymer is expected to be nearly as mobile as a corresponding low M LC, hence the absence of liquid crystal deficiency and effects related to perfectioning. On the other hand, in the more mobile 9.11 copolymer the imperfections produced in the first place are also expected to be less severe, hence the altogether lower deficiency in the degree of liquid crystallinity which is the experimental observation. As already stated, analogous considerations apply to the effect of molecular weight, higher molecular weights implying lower mobility and vice versa. In our comparison between 5,7 and 9.11 the two effects are combined. It follows from this combination of factors that the variability in the non-equilibrium state of liquid crystallinity, as normally observed, is most pronounced at intermediate chain flexibilities and molecular weights. Conversely, when little variability is observed the sample may either be near liquid crystalline perfection (as with high flexibility and low M) or furthest away from perfection (low flexibility, high M), but in the latter case not responding to perfectioning influences. For a more all embracing comparison, however, compounds of identical molecular weights but differing flexibilities would need to be systematically compared, and also comparison would have to be made for annealing both above $T_{m_{max}}$ (i.e. in the LC state) and below (i.e. in the crystal state) a procedure currently in progress.

iii) Perfectioning is a multistage process. At least two stages have been identified: an initial fast and subsequent slower process, both of which can be approximated as exponential functions in time.

iv) Grain structure. As before, the perfectioning of the state of liquid crystallinity is accompanied by the coarsening of an optically identifiable microstructure. We believe that the dark "grain boundaries" correspond to a network of disinclinations which, if correct, would be the course of liquid crystal deficiency registered by DSC. Somewhat

disappointingly, in the presently studied 9,11 copolymer this coarsening was not as marked as with 5,7 previously. While consistent with smaller changes in "degree of liquid crystallinity" (if not obviously with its absolute value on which we have no information so far) the finer scale of the texture makes detailed analysis of images (as intended during the last period) more difficult. We believe this finer structure is associated with the higher molecular weight of this particular material. It is clear that for larger scale textures and for heightened opportunities in the exploration of the microstructure we need to turn to shorter chain polymers, which will be undertaken.

Comonomer Composition Ratio

As a further line in the area of non equilibrium liquid crystal deficiency we are currently exploring the effect of comonomer composition ratio for the copolymer system 9.11, including homopolymers 9 and 11 with several copolymer compositions in between. At this stage of the work we examined the series after annealing within the liquid crystal range (i.e. at $T_m < T > T_i$) and determined T_i and ΔH_i i.e. temperature and enthalpy of isotropization respectively. The annealing was at identical temperatures for the same fixed time for all samples aiming to obtain high perfection of liquid crystallinity. So far there is no guarantee that the maximum perfection has in fact been obtained in all: for this the full kinetics would need to be studied as it has been for the 60-40% ratio previously (Figs 5-6). Even so, at this stage a remarkable trend has emerged and will be reported in what follows.

Fig. 8 depicts T_i and ΔH_i as a function of 9-11 comonomer ratio. T_i is a monotonically increasing function of 9 content, while ΔH_i has a pronounced maximum. Thus the fact that the nematic structure of the copolymer of broadly equal comonomer composition has greater stability than in the corresponding homopolymers is apparent. The reality of the latter assertion can be seen even qualitatively from the thermograms in Fig. 4b) showing the starting and end states of annealing for homopolymers 9 and 11. The smaller effects of perfectioning compared to their 60:40 copolymer (fig. 4a) is apparent.

The effect of a maximum in ΔH_i is unexpected. Even if we had the situation that the homopolymers have not had the chance to perfect themselves to the same extent as the copolymers at or close to the maximum under the annealing treatment given, the fact remains that the copolymers in question have at least the ability for greater perfectoning, whether this is in absolute terms or only in rates. A plausible explanation could lie in the higher entropy of the corresponding molten state, an alternative to the actual higher perfection of the nematic state, due to larger entropy of mixing of the dissimilar comonomer units present in comparable amounts. Even so, the fact that T_i does not follow the same trend would require further scrutiny. Whatever the ultimate cause, this new issue is clearly most relevant for purposeful liquid crystal polymer design and is being further investigated.

II ORIENTATION OF LYOTROPIC RIGID MOLECULES (PBT)

Background and Objectives

During the present period we returned to one of our previous main themes, the orientation of rigid molecules in general and orientability in the liquid crystalline state in particular. The importance of this topic is evident: liquid crystal forming polymers are amongst the most advanced materials to date and orientation and orientability are respectively crucial stages and parameters in their processing, also determining the ultimate properties of the final product.

The material we used is polybenzbisthiazole (PBT) with which we have had previous experience[5,6,7]. It is being processed in the lyotropic state and is amongst the strongest material known to man. It is both a model for other materials of its class (including Kevlar and alike) and is important in its own right.

The broader objective was to follow orientational behaviour under externally imposed orienting influences. Methodology to achieve orientation in the liquid state has been developed in this laboratory previously together with its registration through birefringence. To this method of registration, thanks to developments during the present period, we are now adding X-ray diffraction, with its superior information conveying capabilities.

The particular aspect of orientational behaviour, we are addressing here, is the process of disorientation following preceding alignment in the initially ambient nematic state. This topic was chosen for assessing and developing the new X-ray method for two specific, interrelated reasons. First, the ultimate properties of any wet spun produce (lyotropic or otherwise) are determined (or limited) by the disorientation (or molecular relaxation) which takes place during the time that elapses between the the dope leaving the spinaret and solidifying, say, in a coagulation bath. Understanding and ultimately controlling this reorientation is therefore crucial. Secondly, it is a common finding that products from solidified oriented mesophases possess a sharply banded transverse structure (e.g. ref. 8) as revealed by the polarizing microscope which in general are detrimental to ultimate properties. Such banded structures are ubiquitous in both synthetic materials and in structural materials in nature (collagen) and constitute an important level of the overall structure hierarchy. While its origin is totally unclarified, we ourselves have reason to believe that is is a consequence of a cooperative relaxation of previously aligned rigid molecules, and as such is likely to be illuminated by the presently undertaken study on disorientation processes.

Systems

We chose to study PBT in a dope of polyphosphoric acid, in the first instance of 10% concentration. Not only is this a solvent of potential interest for this system but also its very high viscosity lengthens the time-scale of the orientation - disorientation processes which is of great help to in situ studies of these phenomena.

For the present study the dopes were placed between two mica sheets and sheared by displacing the sheets with respect to each other, controlling strain and strain rate, while placed on a preheated surface of appropriate temperature. After shearing, the cell was rapidly sealed with paraffin to avoid coagulation under the influence of moisture. The cell thus prepared, remaining transparent to X-rays, was then placed in a special home constructed X-ray camera, for recording of wide angle X-ray patterns.

Methods of Study

Two types of X-ray information may be anticipated. The first corresponds to diffraction from a one-dimensional periodic system, such as represented by the chemical repetition along a perfectly straight rod. Such an X-ray signal has in fact been found by us in the form of sharp reflections (00ℓ) in the highly oriented nematic liquid crystalline state, and is at the centre of ongoing study. This provides the most direct possible information on the rigid chain orientation irrespective of whether the chain is in a liquid crystalline state or not. The second type of diffraction information is expected from diffraction due to lateral packing of rods: this should arise in the liquid crystalline

state in the form of broad haloes. So far we have not obtained such, but hopefully we anticipate to do so in the future.

As all signals are transient, extremely high intensity X-ray sources is required. We were fortunate to have access to the Daresbury Synchrotron source. Thanks to this we succeeded in recording successive stages of disorientation photographically through the spread of the meridional (00ℓ) X-ray reflection (Fig. 9). This together with the evaluation of the patterns represent a major technical advance setting the scene for future developments currently in process.

Evaluation of diffraction patterns: Software development;

First results

Full utilisation of the diffraction images required extensive development of information processing. Again we were fortunate in having access to the top ranking facility an Optronics Photoscan P1000 microdensitometer with the help of which X-ray patterns recorded on film were digitised. All the software to analyse the raw binary arrays as outputs by the densitometer, were developed in our laboratory. This includes the following routines:

1) Routine for colour coding and displaying the images using the high resolution Ramtec graphics, (two examples for present topic are shown in figs 9a and b).
2) Routines for finding the image centre (both for images with circular or with lower symmetry).
3) Routine for producing radial scans of the image at specified azimuthal angle intervals, including circular averaging over the whole or over limited sections of the pattern.
4) Routine for further processing the radial intensity data (geometrical corrections, smoothing, fitting, integration, averaging
5) Routine for determining polar distribution and orientational parameters (still under development).

Figures 10a and b show the digitised and colour-coded X-ray diffraction pattern of the 10 per cent PBT solution in polyphosphoric acid (nematic liquid crystal state) after shearing. The mid-exposure times elapsed after shearing are 8 minutes and 15 minutes, respectively. The intense diffuse ring is due to solvent, while the weak inner meridional arcs are due to the intra-molecular periodicity of PBT molecules. The relaxation of orientation with time is indicated by the increased spreading of the meridional arcs.

The radial scans through patterns 10a and b, taken at azimuthal angle (α) intervals of 10 degrees are displayed in Figs 11a and b. E and M denote equatorial and meridional scans ($\alpha=90^{\circ}$ and 0°, respectively). The scans were averaged with their 180° counterparts. The PBT peak of 6.0Å is more widely spread across the azimuthal range in Fig. 10b as compared with Fig 10a. Another interesting feature is the evidence of biaxial preferred orientation of the solvent: the 4.2Å diffuse peak has a maximum both at the equator and at the meridian. Such an effect of preferred orientation of solvent molecules in lyotropic polymer systems has to our knowledge not been reported previously. Its origin is most likely to lie in solvation: i.e. in the preferential orientation of solvated molecules with respect to the polymer chains. In view of the fact the solubilization of such very stiff molecules is an important practical issue, difficult to approach, the above type of information should be highly welcome in this field. Such effects cannot be observed by the usual method employed in similar studies, i.e. optical birefringence, since the latter does not distinguish between the individual contribution of the solvent and the solute. Thus the advantage of the X-ray scattering method is clearly illustrated in this example.

The second advantage of the X-ray method is that it gives the full orientational distribution, rather than just a single orientational parameter. Our method enables the determination of the orientational distribution even from weak and poorly resolved scattering maxima such as are obtained from solutions.

Our programs perform automatic background curve fitting and subtraction prior to integration, as illustrated in Fig. 12. The background-subtracted PBT peak at different azimuthal angles is displayed in Figs. 13a and b for the 8 minute and 15 minute pattern. The orientational broadening is made very clear in these patterns. Integration is now performed and the azimuthal distribution of the integrated intensity of the PBT peak is shown in Fig. 14.

The programme that is still under development will calculate the polar distribution and the orientational order parameter. By observing the time dependence of the latter we shall be able to extract the relaxation times etc., both of the polymer and of the solvent. Even more importantly, the change in the shape of the orientation distribution function could be followed, providing a criticial experimental test for the theoretical predictions on the rotational diffusion in rigid chain systems.

Work along all of the above lines is being vigorously pursued while writing this report and orientation-retraction characterisation of the lyotropic molecules by X-ray diffraction is now, thanks to the above developments, fully in hand. For this work a new shearing cell has been developed (Fig.15) through which both shear and shear rate can be controlled during time resolved in situ X-ray examination with the synchrotron X-ray source. Birefringence is also measurable simultaneously, enabling, for the first time, the two types of information to be correlated. (Preliminary measurements of birefringence have been given in an earlier report (Sept. 1985 - March 1986). The new cell is equally applicable to thermotropic systems which will also be embraced in the nearest future.

III MICROSCOPIC CHARACTERISATION; REGISTERING MOLECULAR STRESSES

This is a new methodological departure of great promise initiated during the present period. It is being announced here in the first place in view of its unique potential for the study of structure hierarchy in its widest generality: it is to link the study of microstructure with the microscopic distribution of molecular stresses under macroscopic loading. Secondly, and more specifically, some of our preliminary tests are on PBT, tapes and fibres, a material featuring in the present report. Our illustration here added refers to this special case (Fig. 16).

The method is a Raman spectroscopic one consisting of two distinct facets. 1) Recording molecular stresses produced by external loading as frequency shifts of appropriate bands in the Raman spectrum. 2) with the aid of a special microscope facility to collecting spectra from microscopically identified regions down to sample volume of $(1\mu)^3$. Combination of 1) with 2) thus should allow the stress distribution in an inhomogeneous sample to be mapped. The inhomogeneity can be due: i) to different structure features of the same material, down to $(1\mu)^3$ level, hence making the technique a method 'par excellence' for the characterisation of structure hierarchies, not only in terms of structure, but also in that of stress response. ii) to different materials contained by the sample in a dispersed state: in brief the method provides a new lever to composites as conventionally defined. In this case stress distribution can be mapped across discrete particles (fibres, fillers) and across the polymeric matrix including features in the self structure of the latter ((i) above), and the interface between the two within the resolution stated.

The above method in its present form has been first announced elsewhere [4]. We then recognized that we ourselves are in a position to pursue it as addressed to our own problems. In the first place we possess the equipment and expertise, with spectroscopic resolution capabilities superior to those in above reference. Secondly, we have our own specific background, to which the method should be applicable in a way which is characteristically our own. The prospects arising therefrom are formulated in a new proposal [1] of ours pointing beyond the duration of the present contract.

In view of our existing involvement with PBT (previous chapter of report) and our preexisting background on PBT fibres (5-7) we are using PBT (amongst other polymers not being reported on here) in our preliminary assessment of the technique and its capabilities. Fig. 16 shows a region of the Raman spectra with and without loading taken of a microscopically selected region of a fibre. The shift in frequency (which under circumstances can be several times as large as in Fig. 16 - ref. 4 and our own work in progress) is apparent. Amongst others it lends itself to the question as to which specific bonds are loaded within the monomer repeat unit, in addition to which molecules are load bearing with respect to the microstructure. The prospects arising from the combination of these two enquiries against the background of the rest of the programme appear to us exciting and unlimited which we are uniquely placed to exploit.

RESEARCH PLANS

Plans envisaged fall in two broad categories: pursuance of topics and new opportunities arising from work during present period and reversion to some of the earlier subjects temporarily shelved during the present period. Here all these subjects will be listed, the extent they will be pursued depending on acquisition of new materials, specifically, newly synthetized polymers from Cleveland (Prof. Percec) and access to special facilities such as the synchrotron X-ray source. We have optimistic expectations regarding both.

Non-equilibrium degree of liquid crystallinity. With imminent advent of more new materials (Prof. Percec) the presently pursued correlations with chain flexibility and molecular weights will be finalized. Concurrently, renewed attention will be given to the relation between microscopically visible grain texture and calorimetrically measured liquid crystal deficiency. In the course of it, identification of the nature of the grain boundaries (presumed to be disinclinations) will be attempted, and if possible quantified. Beyond that, their relation to structure hierarchies, as seen in the truly crystalline state, explored.

With the advent of suitable new materials we shall revert to the exploration of lyotropic - thermotropic phase diagrams thus linking lyotropic with thermotropic LC materials. Promising advances have been made previously but we thought it prudent to await a supply of wider range of compounds before resumption of further work now to be undertaken.

On the crystallographic scale of the structure hierarchy, work during early periods on mesogen-spacer stacking modes will be resumed with the aim of linking up with higher level structural hierarchies. Most significantly, we shall utilise our Raman spectroscopic molecular stress registration (see below) by which the loaded portion of the mesogen spacer sequence should become identifiable, which in turn should correlate with the scheme of mesogen spacer packing established during previous periods.

Orientability in the thermotropic and lyotropic states. Thanks to the technique development work during the present period we are now in a position to follow orientation and relaxation in the nematic state by an X-ray method determining molecular orientation directly. This will be pursued in the lyotropic state, to be followed by analagous studies on thermotropics under controlled strain and strain rates. It is planned to correlate this work with the concurrent registering of structures and their changes on the optical level of the structure hierarchy, thus linking up with them the topical issue of "domains" in LC flow and appearance of transverse bands on relaxation.

Raman spectroscopic molecular stress registration, referred to above in connection with mesogen-spacer stacking, will be pursued in broadest generality. In particular, it will be extended to microscopic stress distribution mapping across wide ranges of structure hierarchy in an attempt to bridge structure studies with studies of mechanical properties. This line of work is of still unforeseeable promise and given the opportunity will be carried over to a future grant period as stated in new proposal [1].

References

1. A. Keller, J.A. Odell, ERO proposal submitted January (1988).
2. J.L. Feijoo, G. Ungar, A. Keller, A.J. Owen, V. Percec, J. Molecular and Liquid Cryst. in the press.
3. J.L. Feijoo, G. Ungar,A. Keller, V. Percec in preparation.
4. R.J. Day, I.M. Robinson, M. Zakikhoui, R.J. Young, Polymer, 28, 1833 (1987).
5. J.A. Odell, A. Keller, E.D.T. Atkins, M.J. Miles, J. Materials Sci. 16, 3309 (1981).
6. J.A. Odell, A. Keller, E.D.T. Atkins,J. Polymer Sci. Letters, 21, 289 (1983).
7. J.A. Odell, A. Keller, E.D.T. Atkins,Macromolecules, 18, 1443 (1985).
8. C. Vinay, A.M. Donald, A.H. Windle, Polymer, 26, 870 (1986).

Figure Captions

Fig. 1 Transition temperatures of 5,7 copolymer (50:50) as a function of molecular weight. T_g = glass transition, T_m^{max} max crystal melting point, T_i = isotropization temperature. (o as prepared o on heat treatment in M ranges where non-equilibrium liquid crystal deficiences pertain).

Fig. 2 Free energy (G) v. temperature T diagram (schematic). C = crystal, LC= equilibrium liquid crystal, L = isotropic liquid with a particular state of non-equilibrium liquid crystal (broken line) indicated.

Fig. 3 T_i v. annealing time for 5,7 copolymer.

Fig. 4 a) DSC thermograms of 9,11 copolymer, (60:40) M_n = 30800 after times of annealing at temperature T, $T_{max} < T < T_i$ (solid line). The broken line corresponds to an annealing temperature in the crystalline state ($T < T_{max}$) for terminal time.

b) Same for homopolymers, 9(A,B) 11(C,D) corresponding to unannealed and a strongly annealed sample (lower and higher temperature peaks in corresponding pairs respectively).

Fig. 5 T_i v. annealing time for copolymer 9,11 above T_m^{max}. Solid line experimental, broken line best single exponential fit. Calculated T_i^{∞} = 171.6°C.

Fig. 6 Heats of isotropization (ΔH_i) and "degrees of liquid crystallinity" ($\Delta H_i(t)/\Delta H_i^{\infty}$) as a function of annealing time, for annealing in the liquid crystal state. Copolymer 9,11.

Fig. 7 Grain structure as seen under the polarizing microscope of copolymer 9,11 (60:40). Unannealed (top); after annealing in the LC state (bottom).

Fig. 8 ΔH_i and ΔT_i v. composition (9:11 ratio), in copolymer (9,11). The samples were annealed in the LC state for fixed times and temperatures chosen so as to ensure significant perfectioning without risk of degradation.

Fig. 9 X-ray scattering pattern of the PBT solution in polyphosphoric acid recorded 7.5 minutes (mid-time) after shearings. Shearing direction vertical. The weak inner meridional arcs are due to PBT backbone periodicity. The outer halo is mainly due to the solvent.

Fig. 10 Digitised and colour coded X-ray scattering patterns of sheared PBT solution: a) 7.5 minutes and b) 15 minutes after shear had ceased. Fig. 10a shows the same pattern as that in Fig. 9.

Fig. 11 Radial scans of X-ray scattering patterns in Figs 10a and b (Figs 11a and b, respectively). Scans shown are of 10 deg. intervals of the azimuthal angle β, each scan being an average of 20 scans at 1 degree intervals recorded in the range $\beta-5<\beta<\beta+5$ and $\beta+175<\beta+180<\beta+185$. M = meridional, E = equatorial.

Fig. 12 An example of automatic background fitting of an 8th degree polynomial under the PBT backbone peak in a radial scan of Fig. 11.

Fig. 13 Background subtracted PBT backbone peak as a function of azimuthal angle β for PBT solution 7.5 minutes (a) and 15 minutes (b) after shear (cf. Fig. 10a and b, and 11a and b). Randomization of initial orientation with time is clearly visible.

Fig. 14 Integrated intensity of the PBT backbone peak vs. azimuthal angle for patterns recorded at 7.5 (crosses) and 15 minutes (squares) after shear (cf. Fig. 13 a and b). Integration limits: 5.2 and 7.0Å. 0° refers to the meridional and 90° to the equatorial scan.

Fig. 15 Newly constructed shearing cell for liquid crystal orientation work by X-ray diffraction.

Fig. 16 Raman spectra. A stress sensitive band with sample (a) without load b) loaded.

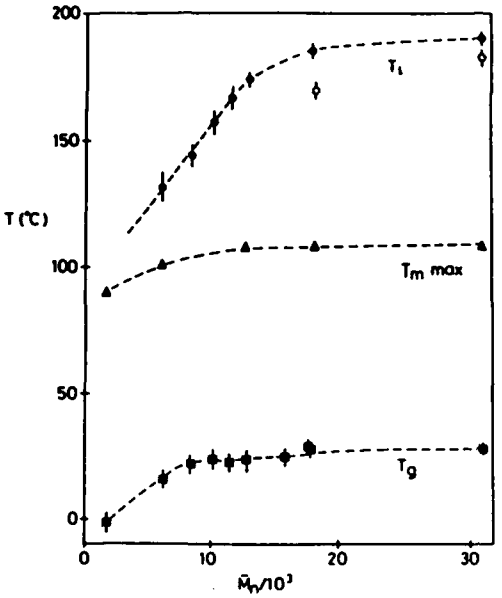

Fig 1

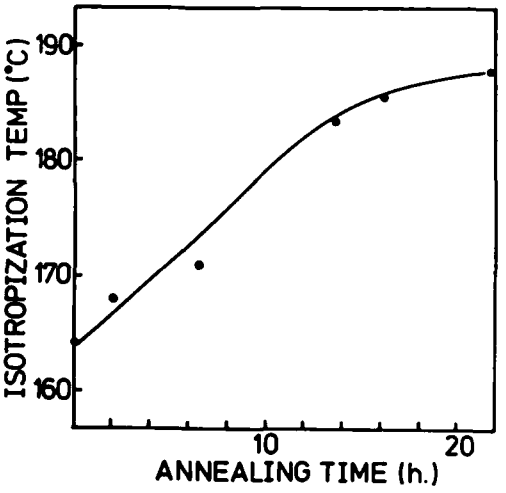

Fig 3

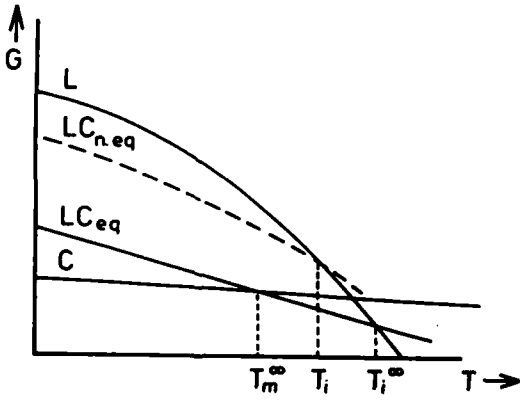

Fig 2

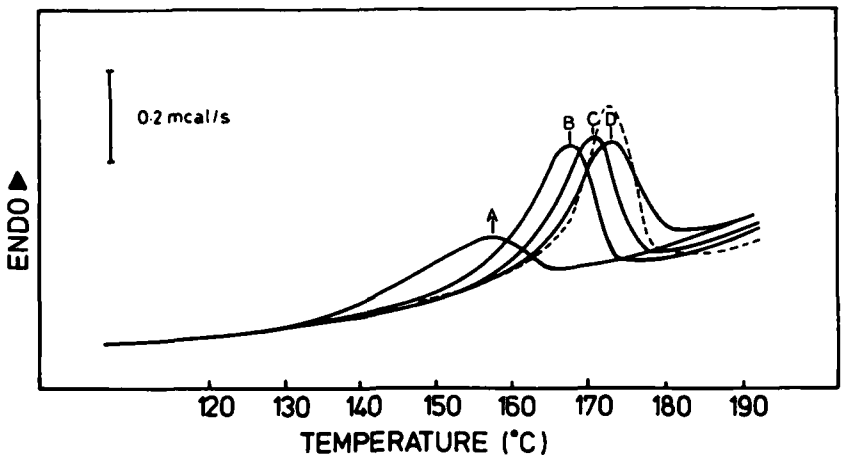
0·2 mcal/s
ENDO
A
B
C
D
120
130
140
150
160
170
180
190
TEMPERATURE (°C)

Fig 4a

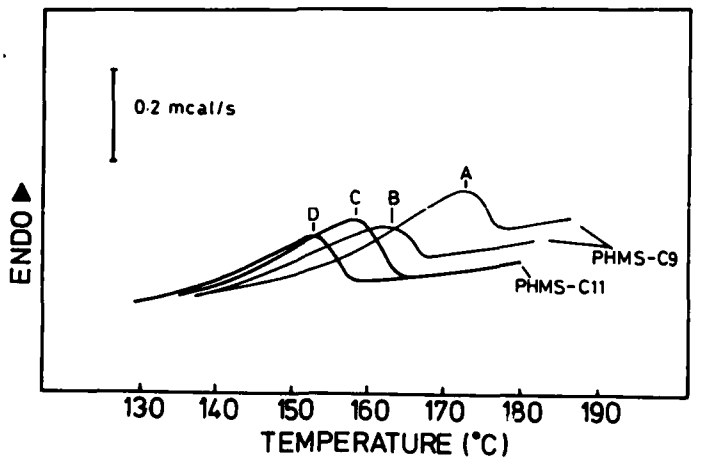
0·2 mcal/s
ENDO
A
B
C
D
PHMS-C9
PHMS-C11
130
140
150
160
170
180
190
TEMPERATURE (°C)

Fig 4b

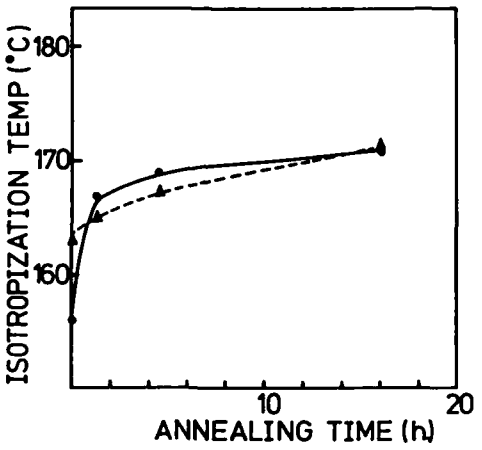
ISOTROPIZATION TEMP (°C)
180
170
160
10
20
ANNEALING TIME (h)

Fig 5

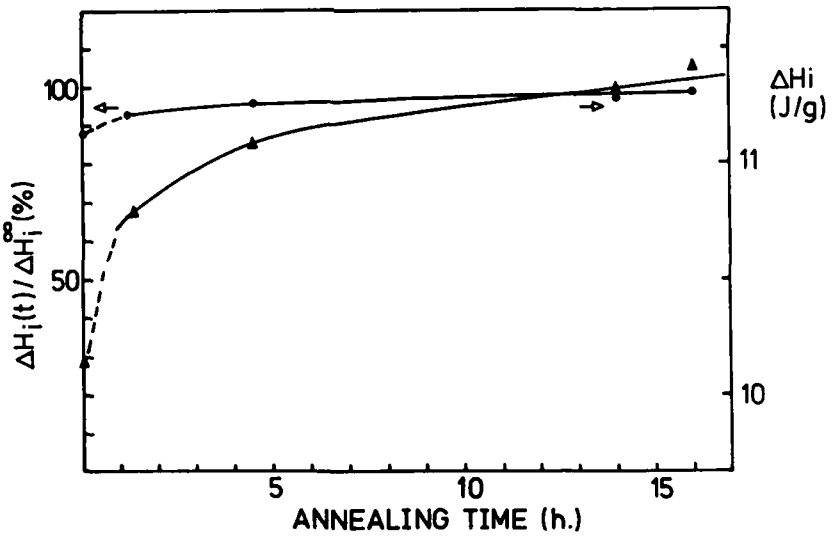
100
50
$\Delta H_i(t)/\Delta H_i^{\infty}$(%)
ΔHi
(J/g)
11
10
5
10
15
ANNEALING TIME (h.)

Fig 6

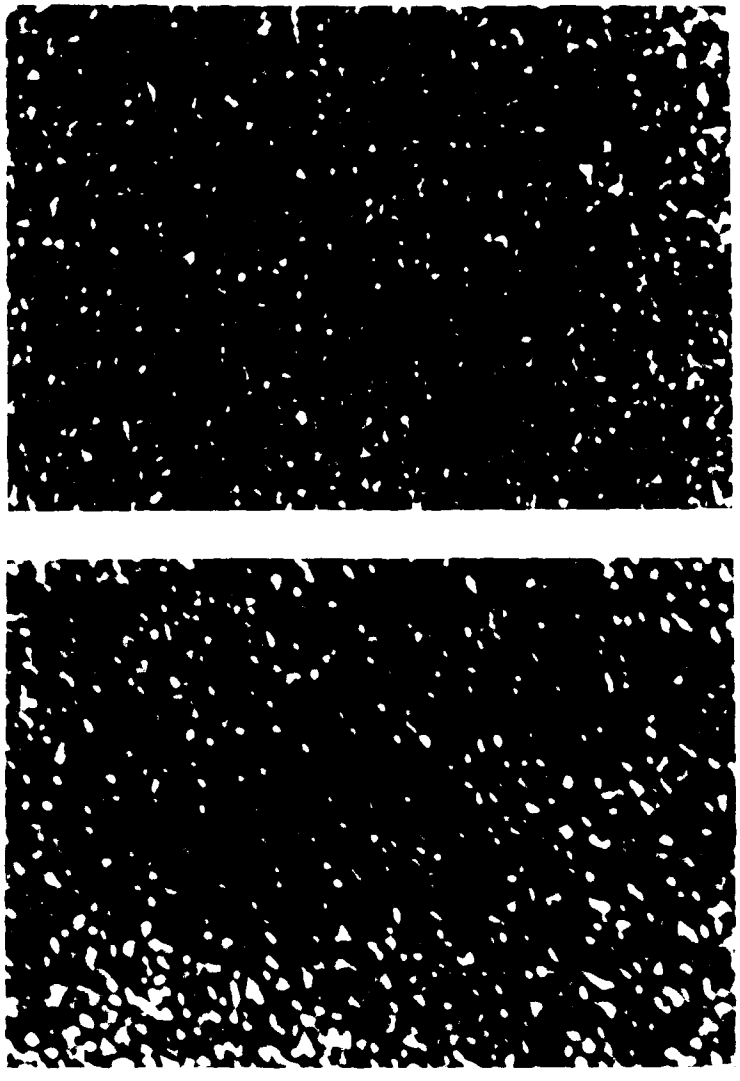

Fig 7

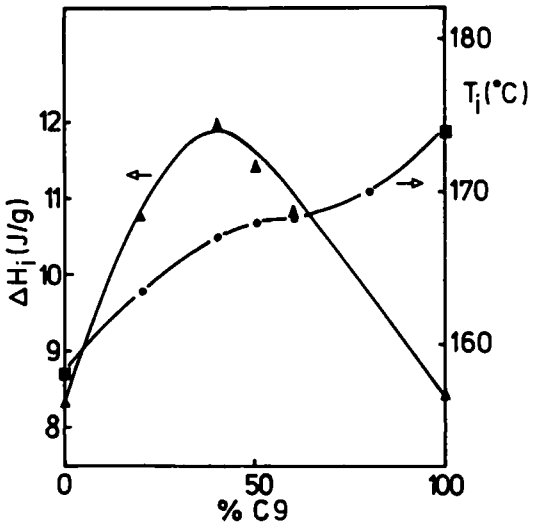

Fig 8

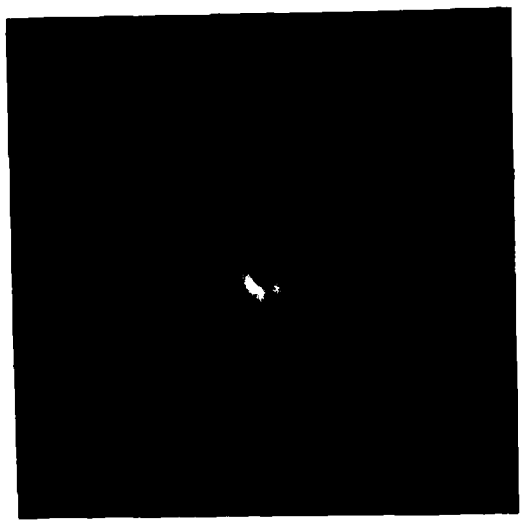

Fig 9

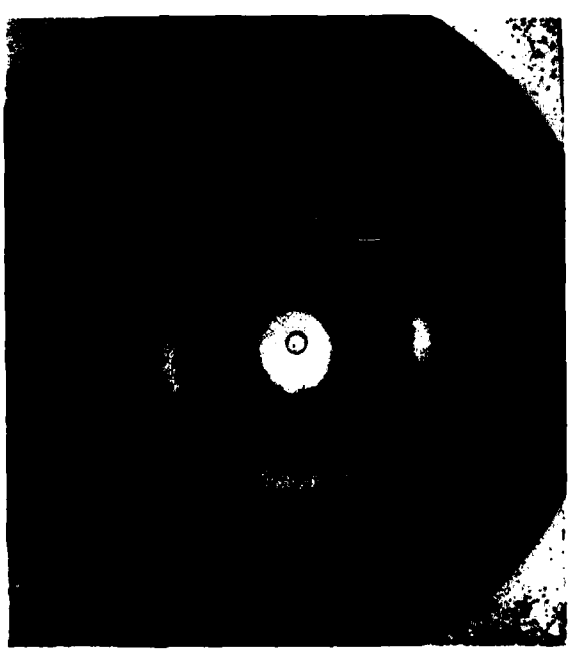

Fig 10a

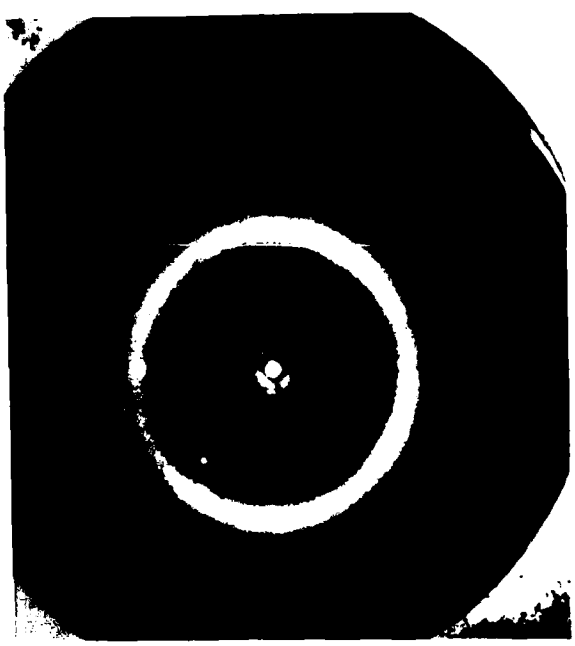

Fig 10b

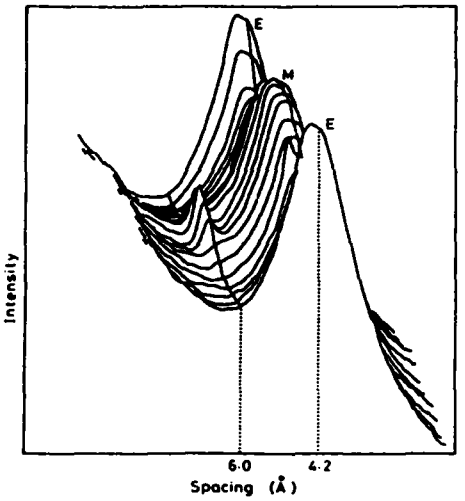

Fig 11a

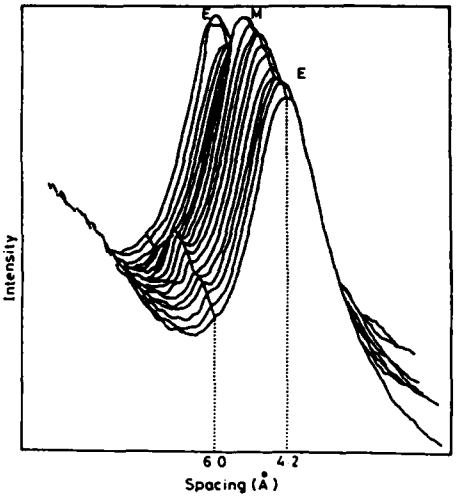

Fig 11b

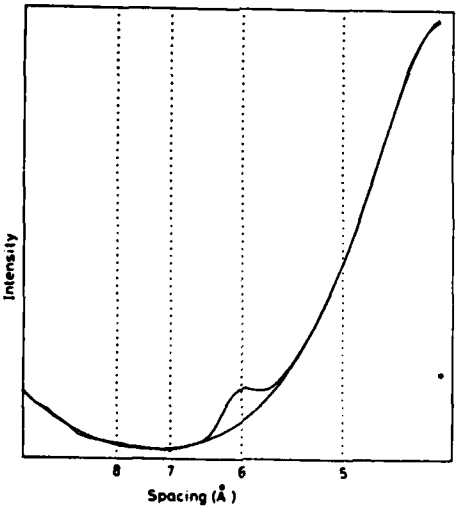

Fig 12

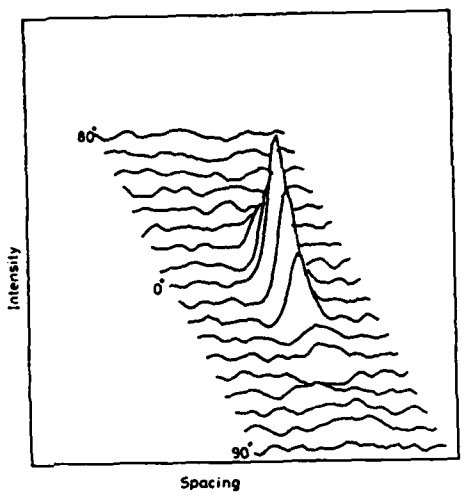

Fig 13a

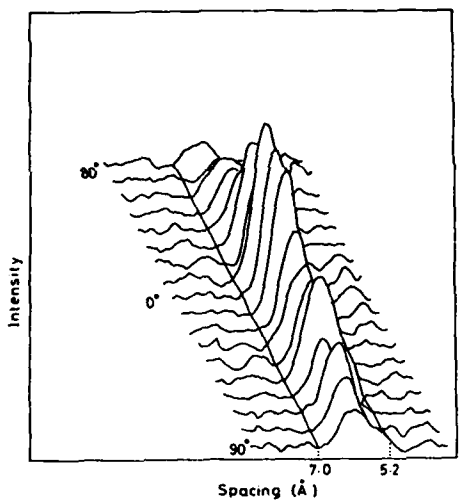

Fig 13b

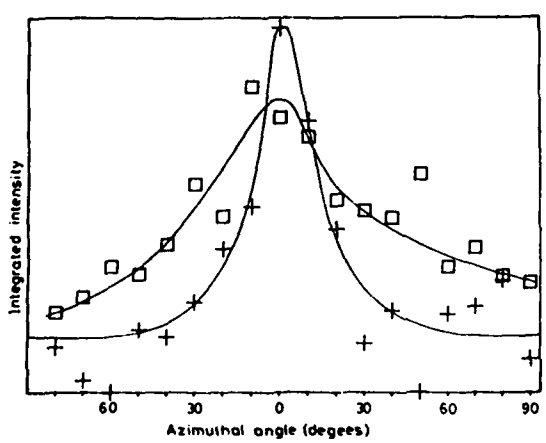

Fig 14

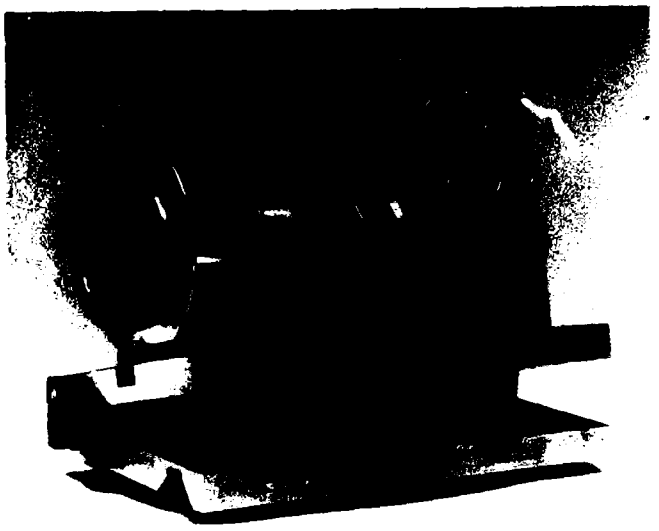

Fig 15

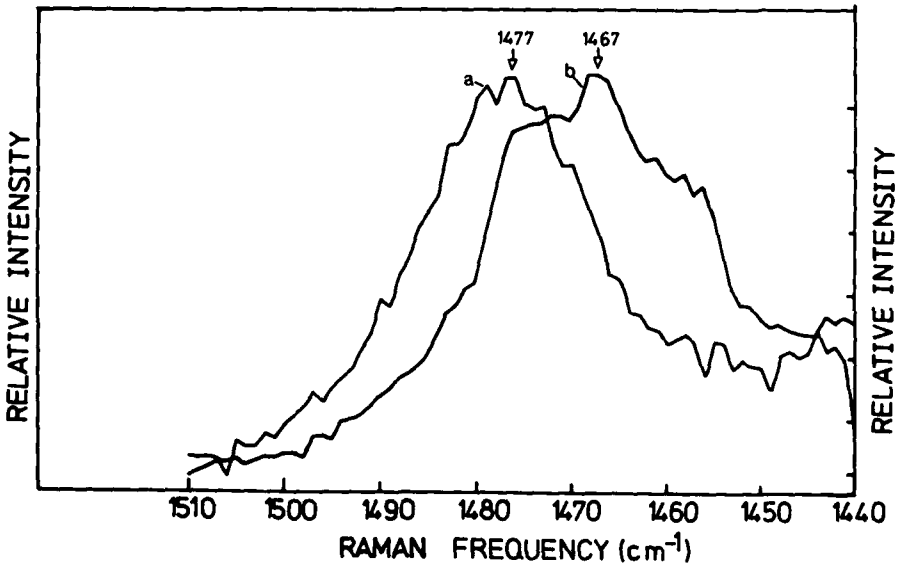
1477
1467
a
b
RELATIVE INTENSITY
RELATIVE INTENSITY
1510
1500
1490
1480
1470
1460
1450
1440
RAMAN FREQUENCY (cm⁻¹)

Fig 16

END

DATE
FILMED

8 8

mesogen spacer sequence should become identifiable, which in turn should correlate with the scheme of mesogen spacer packing established during previous periods.

Fig. 5 T_i v. annealing time for copolymer 9,11 above T_m^{max}. Solid line experimental, broken line best single exponential fit. Calculated T_i^∞ = 171.6°C.